SSI EFFECT ON DYNAMIC CHARACTERISTICS OF LOW & MEDIUM-RISE BUILDINGS BASED ON SIMPLIFIED ANALYSIS AND OBSERVATION

Nobuo FUKUWA[1] **and Jun TOBITA**[2]

1) Professor, Dr. Eng., C-CRAST, Nagoya University,
Furo-cho, Chikusa-ku, Nagoya 464-8603, fukuwa@sharaku.nuac.nagoya-u.ac.jp
2) Assoc. Professor, Dr. Eng., School of Engineering, Nagoya University,
Furo-cho, Chikusa-ku, Nagoya 464-8603, tobita@sharaku.nuac.nagoya-u.ac.jp

ABSTRACT ：Many researchers have indicated that the level of damages caused by recent earthquakes, particularly in case of short and stiff buildings, has been predominantly related to the SSI. The current revision of seismic code in Japan includes evaluation of SSI effect on ordinary buildings. Under such circumstances, it is required to accumulate data on actual behavior of buildings with SSI effect. In this paper, the effect of SSI on the dynamic response of buildings, especially ordinary low and medium-rise buildings, is studied through simple numerical analyses and experimental results of earthquake response observation and microtremor tests.
In the analytical study, effect of SSI on natural period, damping and vibration mode is discussed by SDOF model with sway and rocking motion. In the experimental study, dynamic characteristics of several low and medium-rise buildings with various foundation types and ground conditions were investigated. The transfer functions for the two cases of top/basement (fixed-base) and top/ground (SSI included) show a clear difference in the natural frequency, damping and mode shape due to SSI effect. The loss in the effective input motion is clearly observed for buildings with large foundations.

Keywords ：Low and medium rise RC building, Seismic observation, Input loss, Radiation damping, Seismic force, Aseismic design

INTRODUCTION

In the performance based design, sufficient knowledge on seismic resistant performance of the building is required. Hayashi et al. (2000) evaluated the vulnerability curve of the RC building based on the building damages in Hyogoken-Nanbu earthquake like figure 1. The figure means that the low-rise buildings generally have seismic resistant performance of about 10 times of those assumed in the design stage. The margin of the seismic performance which was not considered in the design may reduce the damage of low-rise RC buildings in Hyogo-ken Nanbu Earthquake. This is also proved through the fact that the damage ratio of high-rise buildings with the small seismic margin is larger than that of low and medium-rise buildings. The difference of the seismic margin according to the height of the building can be understood as the followings.

1) With the decrease in the height of building, SSI effects such as input loss and radiation damping increase because of short natural period of the building.
2) And the elastic deformation and rocking motion decrease, while the sway motion with large radiation damping increases.
3) The low-rise buildings generally have many secondary structural members which are not counted

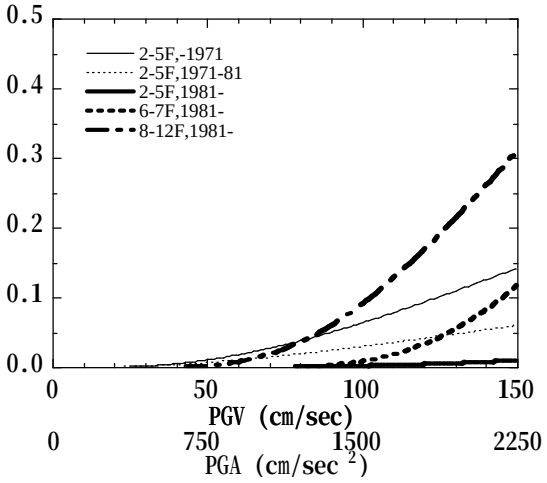

Figure 1 Vulnerability curves for RC buildings except for piloti type ones after Hayashi et al. (2000)

in the structural design.

It is important to quantitatively grasp the margin due to SSI of the middle & low rise buildings in order to promote the performance based design. Here, through the simple SSI analyses and the study of seismic observation results and microtremor data, the general effects of SSI on the dynamic behavior of the middle & low rise buildings are examined.

INERTIA INTERACTION EFFECT BASED ON SIMPLIFIED NUMERICAL ANALYSIS

In order to examine the SSI effects on seismic forces applied to super-structure, the reduction of seismic forces due to SSI are quantitatively evaluated using simplified analysis. Here, *n*-story building with identical mass *m* and floor height *H* is selected for the analysis. When assuming the linearly increase mode shape for first mode and the natural period proportional to number of story ($T=an$), the distribution of stiffeness of super-structure is given by,

$$k_j = \frac{2mp^2}{(an)^2}\left(n(n+1) - j(j-1)\right) \quad (1)$$

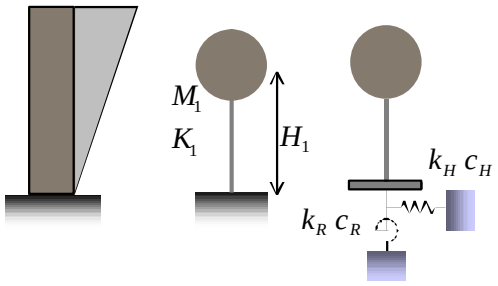

Figure 2 Model for analysis

and the element of first mode participation vector is given by ,

$$bf_j = \frac{3j}{2n+1} \quad (2)$$

When using these relationships, the effective mass M_1, height of mass H_1 and stiffness K_1 of equivalent single degree of freedom system (SDOF) for first mode are derived like,

$$M_1 = nm\frac{3(n+1)}{2(2n+1)} \quad (3)$$

$$H_1 = nH\frac{2n+1}{3n} \quad (4)$$

$$K_1 = m\frac{3(n+1)}{2(2n+1)}\frac{4p^2}{a^2 n} \quad (5)$$

In order to include SSI effect to SDOF system, the springs and dashpots for sway and rocking motion are added beneath the SDOF system. And the mass and moment inertia of the foundation are neglected for simplification. Under this condition, the equivalent SDOF system considering SSI can be written by,

$$\left(-w^2 M_1 + \bar{K}_1\right)u(w) = -M_1 \ddot{Y}_g(w) \quad (6)$$

where, the equivalent stiffeness is expressed by,

$$\bar{K}_1 = \frac{1}{\dfrac{1}{K_1(1+2h_S i)} + \dfrac{1}{k_H + iwc_H} + \dfrac{H_1^2}{k_R + iwc_R}} \quad (7)$$

The undamped equivalent natural period and damping ratio are estimated from the followings.

$$\bar{T} = T\sqrt{1 + \frac{K_1}{k_H} + \frac{K_1 H_1^2}{k_R}} \quad (8)$$

$$\bar{h} = \sin\left(\frac{1}{2}\tan^{-1}\frac{\mathrm{Im}\,\bar{K}_1}{\mathrm{Re}\,\bar{K}_1}\right) \quad (9)$$

Here, h_S is structural damping considered by complex damping, k_H, c_H, k_R and c_R are spring constants and damping coefficients for sway and rocking motion. The ratio of elastic deformation, sway displacement and rocking displacement in total displacement corresponds to the ratio of reciprocal of each spring constant respectively, which means the ratio of each term in denominator of equation 7.

Spring constants and damping coefficients for sway and rocking motions are evaluated using the static spring constants of rigid circular surface foundation and the product of mass density, wave velocity and foundation area respectively. For rectangular foundation, the radius of foundation is evaluated by equivalent area for sway

mode and by equivalent moment inertia for rocking mode. These are,

$$k_H = \frac{8Gr}{2-n} \qquad c_H = rV_S pr^2 \quad r = \sqrt{\frac{4bd}{p}} \tag{10}$$

$$k_R = \frac{8Gr^3}{3(1-n)} \quad c_R = r\,\frac{3.4V_S}{p(1-n)}\,\frac{pr^4}{4} \quad r = \sqrt[4]{\frac{16bd^3}{3p}} \tag{11}$$

where, G, V_S, r and n are shear modulus, shear wave velocity, mass density and Poisson's ratio of soil, r is radius of equivalent circular foundation, b and d are half width and half depth of rectangular foundation.

Here, we assume the building with the weight per floor area of 1ton/m^2 (m=0.4bd), floor height of H=3m, constant for natural period of a=0.05. For the square plan building with each floor area of 1000m^2, natural period, damping ratio and deformation ratio are calculated and shown in Figures 3-6. We also assume the Poisson's ratio of soil as n =0.4 and no structural damping ratio.

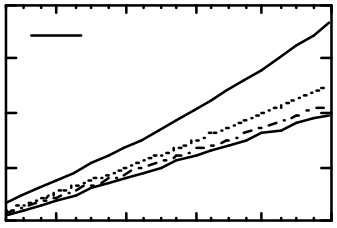

Figure 3 Natural period

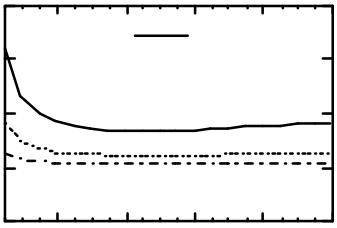

Figure 4 Change of natural period

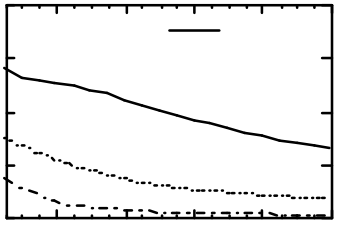

Figure 5 Damping ratio

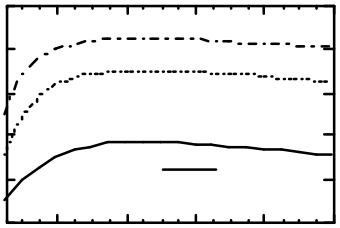

(a) Elastic deformation

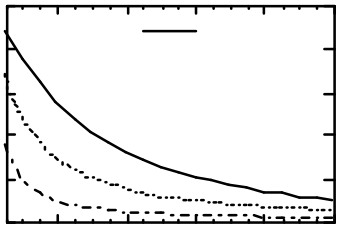

(b) Sway motion

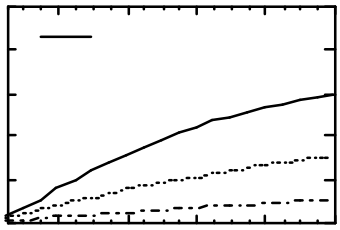

(c) Rocking motion

Figure 6 Ratio of elastic deformation, sway and rocking motion

The figures show the increase of natural period, large damping ratio and contribution of sway mode for low-rise buildings on soft soil. When adopting the commonly used relationships for the damping modification of response spectrum $S(T,h)$,

$$\frac{S(T,h)}{S(T,h=0)} = \frac{1}{1+10h} \tag{12}$$

the response of SSI system with damping ratio of 20% becomes half of standard fixed base system with damping ratio of 5%. On the other hand, in case of tall building, elastic deformation becomes dominant for stiff soil and rocking motion does for soft soil.

The damping shows the tendency of hT=const (hn=const). This tendency can be explained as follows. Assuming that the structure behaves as rigid body and the sway mode dominates, equation 9 for small damping ratio can be approximated like,

$$h = \sin\left(\frac{1}{2}\tan^{-1}\frac{\mathrm{Im}\,K}{\mathrm{Re}\,K}\right) \approx \frac{1}{2}\frac{\mathrm{Im}\,K}{\mathrm{Re}\,K} \approx \frac{c_H w}{2k_H} = rV_S pr^2 w \Big/ 2\cdot\frac{8Gr}{2-n} = p^2 r \Big/ T\cdot\frac{8V_S}{2-n} \tag{13}$$

From this equation, the following relationship is obtained,

$$hT = \frac{p^2(2-n)}{8}\,\frac{r}{V_S} \approx \frac{2r}{V_S} \tag{14}$$

The similar relationship is also obtained for rotational motion,

$$hT = \frac{10.2p}{32}\frac{r}{V_S} \approx \frac{r}{V_S} \tag{15}$$

Comparing Eqs. 14 and 15, the radiation damping for sway mode is about twice of that for rocking mode. The modal damping ratio of coupled system is a value averaging the frequency independent structural damping and the frequency dependent sway and rocking damping expressed by equations 14 and 15 with the weight of each deformation ratio. That is

$$h = \frac{\dfrac{4n(2n+1)Gra^2h_s}{3(n+1)p^2m} + \dfrac{p^2(2-n)^2r}{8V_S\overline{T}} + \dfrac{(2n+1)^2H^2(1-n)}{rV_S\overline{T}}}{\dfrac{4n(2n+1)}{3(n+1)p^2}\dfrac{Gra^2}{m} + (2-n) + 3(1-n)\left(\dfrac{(2n+1)H}{3r}\right)^2} \tag{16}$$

As a result, we know that the damping ratio decreases as the increase of natural period and the magnitudes of damping ratio are ordered as sway > rocking > superstructure. Therefore, for tall building, the damping is reduced by the effect of the small damping due to the slight sway motion as well as the damping reduction effect due to the long natural period. This seems to be one of the reasons for the difference of damage ratio among different height of buildings shown in figure 1.

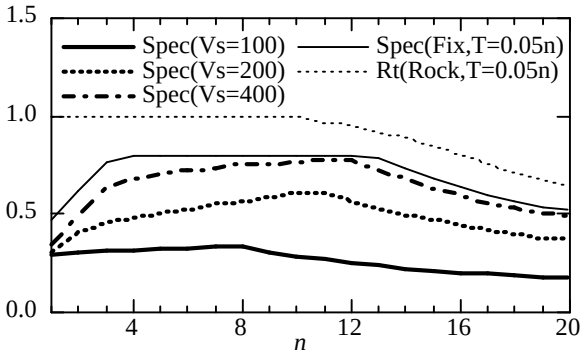

Figure 7 Maximum acceleration response for various soil condition

Figure 7 shows the maximum response acceleration for several soil conditions. The structural damping is assumed to be 0.05. Here, the response spectrum proposed in newly revised seismic code and the equation 12 are used for calculation. In the figure, Rt curve, which defines the seismic force in current seismic code since 1981, is also plotted.

Next, the slender plan building with different structural types for span and girder directions are considered as examples of buildings such as school and apartment house. For span direction, wall type structure is assumed with half width of 7m and α =0.025, while frame type structure with half width of 35m and α =0.075 is selected for girder direction. The results are shown in figures 8-11. In the figures, results of equivalent square building with a=0.05 are compared. The shear wave velocity of soil is assumed to be 200m/s. In case of rectangular plan, rocking motion becomes dominant in span direction while in girder direction sway motion dominates for low-rise building and elastic deformation does for high rise building. The variation of structural type in span and girder directions extends the differences of vibration mode and damping among both directions. From these results, we know the differences in vibration direction of applied seismic forces as well as the seismic performance such as seismic resistance capacity and deformability. In order to grasp the change of seismic forces due to shape of plan, the maximum response accelerations are plotted in figure 12 compared with Rt curves in current seismic code. Here, Rt curve is evaluated using a=0.1. Even for same size building on same soil condition, the seismic forces differs due to structural frame type and shape of plan.

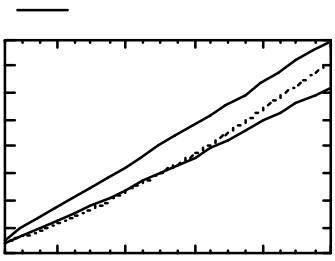

Figure 8 Natural period for rectangular plan

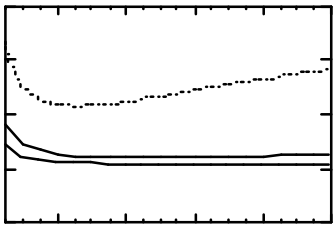

Figure 9 Change of natural period for rectangular plan

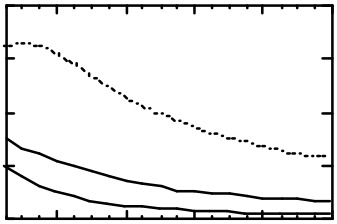

Figure 10 Damping ratio for rectangular plan

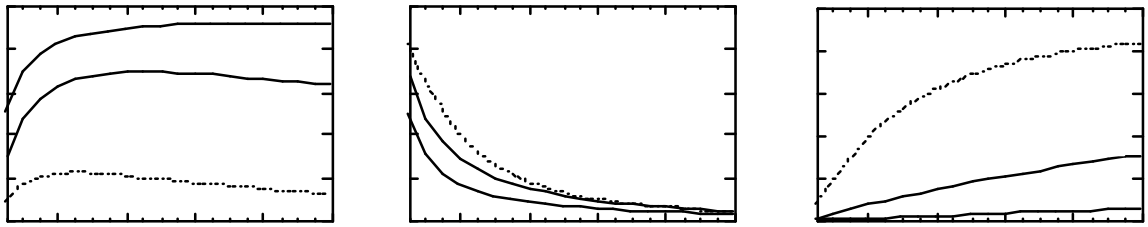

(a) Elastic deformation (b) Sway motion (c) Rocking motion

Figure 11 Ratio of elastic deformation, sway and rocking motion for rectangular plan

INERTIA INTERACTION EFFECT BASED ON OBSERVATION RESULTS

Microtremor and earthquake observation records obtained in several low & middle rise buildings in Nagoya university are examined in the followings in order to verify above-mentioned analytical result. Figure 13 shows a relationship between the modal damping of first mode and the building height based on microtremor records. These are values identified using spectrum fitting technique for transfer function between building roof and ground surface. Filled symbols show results for each construction stage of a 10 story building while open ones for respective buildings. Square symbols show results for longitudinal direction and circles for transverse direction.

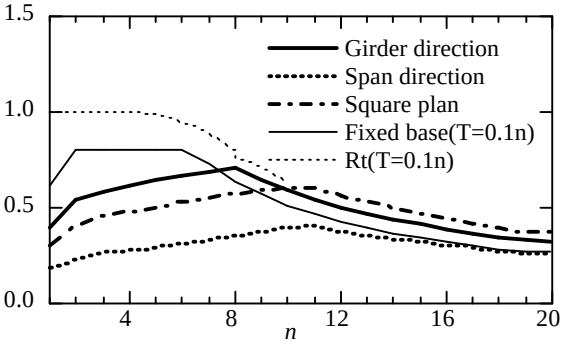

Figure 12 Maximum acceleration response for rectangular plan building

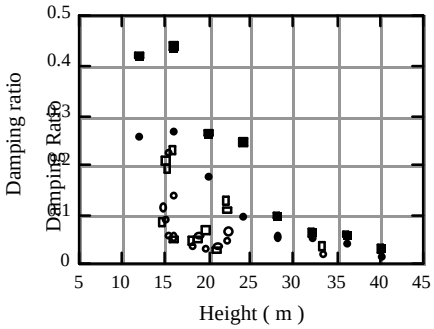

Figure 13 Relationship between modal damping and building height based on microtremor

Figure 14 shows the relationship between the average N value of 10m soil depth and the natural period and damping ratio of 5 and 6 story buildings. The natural period becomes long and the damping ratio increases for softer soil condition.

In figures 15 and 16, the natural period and damping ratio is compared between with and without the SSI. The comparison was done for 10 and 4 story buildings. The results with SSI is evaluated from the transfer function between roof and ground surface, while the transfer function between roof and basement is used for the results of fix-based condition, in which rocking motion is not fixed. From the figures, the effect of frequency reduction and damping magnification by inertia interaction are recognized in the earthquake observation results. Here, maximum acceleration of ground surface distributed from 1 Gal to 100 Gal, so that the effect of amplitude dependency is also included in the results.

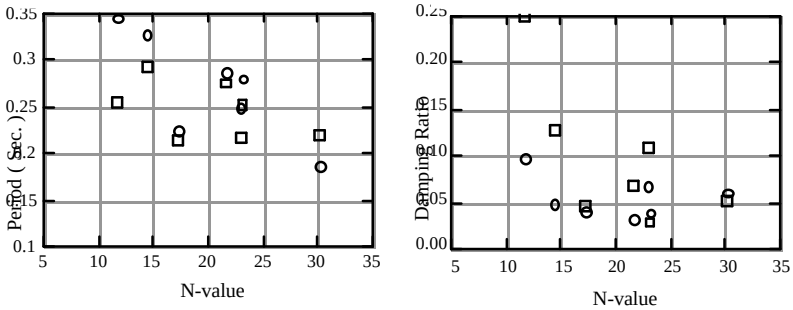

Figure 14 Relationship between the natural period & damping and the average N value of 10m soil depth for 5 and 6 story building

For the reference, the relationship between natural frequency and maximum acceleration for 10 story building is

shown in figure 17. In the design stage, this building had been designed as first natural frequency of 1Hz. That is to say, the actual building has about 3 times the stiffness of that in the design. This seems to be the contribution of nonstructural members. The existence of nonstructural members seems to be another seismic margin of the middle & low rise buildings.

The seismic observation result of neighboring 3 story building and 6 story building, which are 2m apart and connected by expansion joint each other, are not a simple one like in figure 16. As an example, the results of 6 story building is shown in figure 18. This variation of identified results is due to the cross interaction effect. The result varies by the earthquakes and there are cases where the damping is small. When considering SSI effect in the design of the building in urban area, where the building is easy to adjoin, the structure-soil-structure interaction seems to be one of the factor which reduces inertia interaction effect.

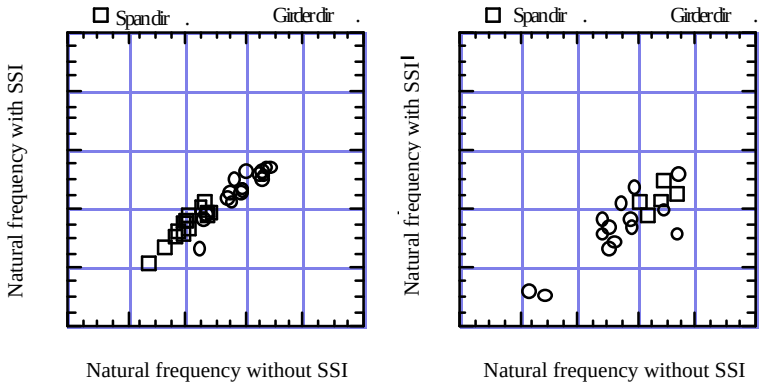

(a) 10 story building (b) 4 story building

Figure 15 Comparison of the natural period with and without SSI

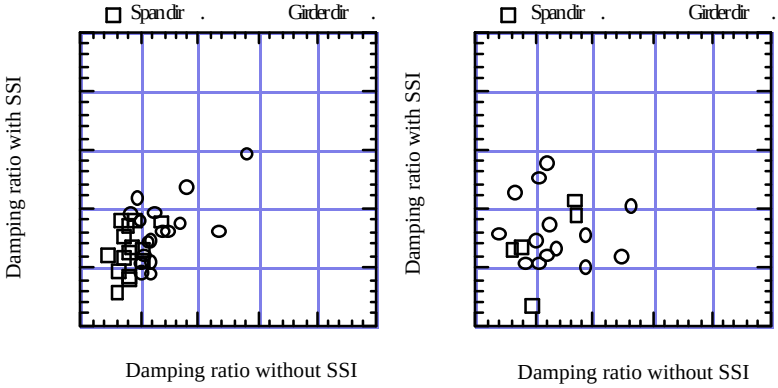

(a) 10 story building (b) 4 story building

Figure 16 Comparison of the modal damping with and without SSI

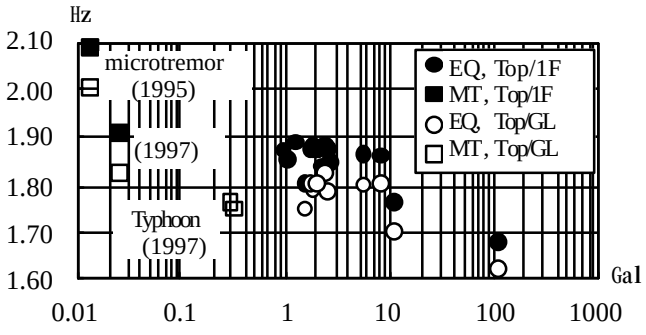

Figure 17 Amplitude dependency of natural frequency for 10 story building

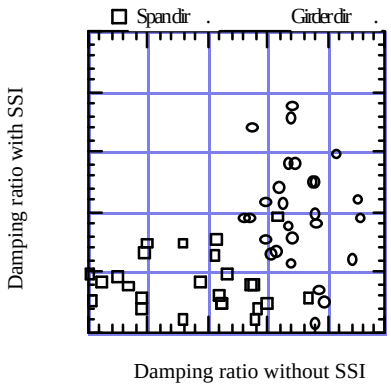

Figure 18 Comparison of the modal damping with and without SSI for 6 story building neighboring 3 story building

KINEMATIC INTERACTION EFFECT BASED ON SEISMIC OBSERVATION

For six buildings observing the seismic strong motion at basement and ground surface simultaneously, the input loss effect is examined. The features of structure and soil condition for the six buildings are summarized in table 1. The 6 story building neighbors with 3 story building.

Table 1 Summary of buildings

no. of story	foundation /pile length	height	structural type	area of basement	averaged Vs
10	pile/45m	39.3	SRC	1502.0	216
4	pile/6m	17.9	RC	1155.0	244
6	pile/12m	22.3	SRC	603.9	245
3	Spread pile/12m	11.4	RC	374.4	289
2	pile/4m	9.0	RC	262.6	270
1	direct	6.5	S	466.1	330

Fourier spectrum ratio between basement and ground surface is shown in figure 19. The result is averaged spectral ratio using 10-20 seismic records. The result based on microtremor is also shown in the figure. There is the clear input loss effect in high frequency range.

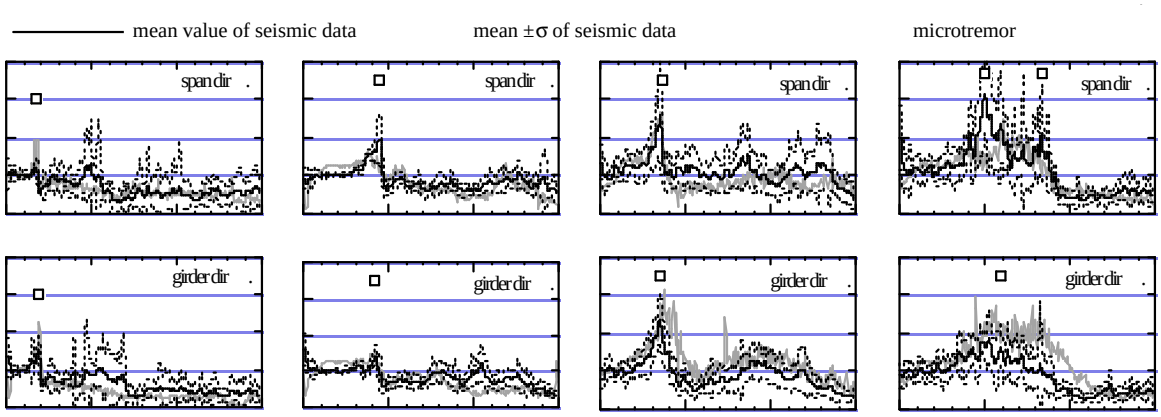

(a) 10F building (b) 4F building (c) 6F building (d) 3F building

Figure 19 Fourier spectral ratio between basement and ground surface for 10, 4, 6 and 3 story buildings

Next, the maximum acceleration ratio between basement and ground surface (PBA/PGA) is examined with the equivalent frequency of ground motion (PGA/PGV/2p) in figure 20. Here, PGA and PBA mean peak ground and basement acceleration, PGV means peak ground velocity. Similarly, the relationship between maximum velocity ratio (PBV/PGV) and the equivalent frequency (PGV/PGD/2p) is presented in figure 21. Here, PGD means peak ground displacement.

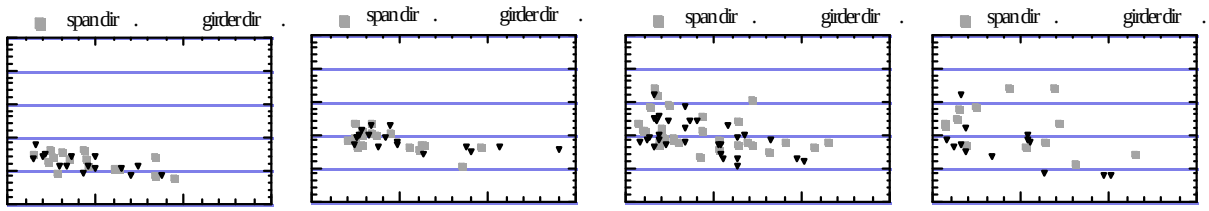

(a) 10F building (b) 4F building (c) 6F building (d) 3F building

Figure 20 Relationship between the maximum acceleration ratio (PBA/PGA) and PGA/PGV/2p

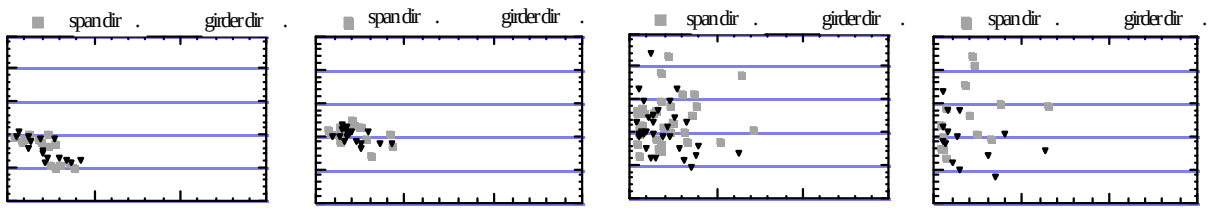

(a) 10F building (b) 4F building (c) 6F building (d) 3F building

Figure 21 Relationship between the maximum velocity ratio (PBA/PGA) and PGV/PGD/2p

Figure 22 shows the relationship between predominant frequency of acceleration Fourier spectrum and the equivalent frequency PGA/PGV/2p while Figure 23 does similar relationship for velocity. The equivalent frequencies are well correspondent to the predominant frequency of seismic ground motion. The response of the basement is reduced in comparison with the ground surface when the equivalent frequency of ground motion is high and the building is large. By defining the equivalent frequency for acceleration and velocity respectively, the similar input loss characteristics are obtained both for the acceleration and the velocity. The

results of figures 20 and 21 look like the Fourier spectrum ratio shown in figure 19. When the adjacent building exists, the results show different characteristics, and the input loss effect is not clearly observed.

In order to uniformly understand above results, the non-dimensional frequency $a_0=2pfB/Vs$ is defined. Here, Vs is averaged shear wave velocity in 10m beneath the surface which is evaluated using N value and regression formula, B is half width of the square foundation with equivalent area, and f is an equivalent frequency of the ground motion. Figure 24 shows the input loss effect on both acceleration response (black dot) and velocity response (gray dot) for all the buildings and all records, where the lateral axis means non-dimensional frequency. The 6 story and 3 story buildings were removed from the figure since the cross interaction effect is included. By using non-dimensional frequency, the common input loss characteristics are obtained.

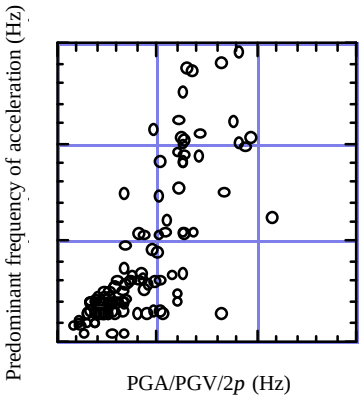

Figure 22 Relationship between PGA/PGV/2p and predominant frequency of acceleration spectrum

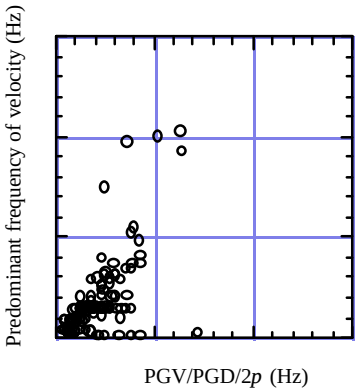

Figure 23 Relationship between PGV/PGD/2p and predominant frequency of velocity spectrum

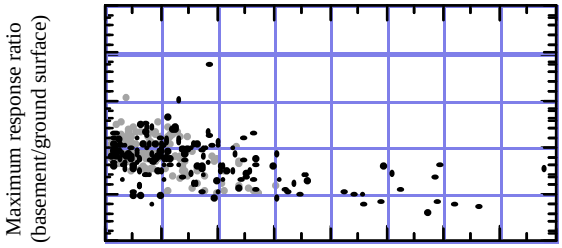

Figure 24 Relationship between maximum response ratio (basement / ground surface) and non-dimensional predominant frequency of ground motion

This result shows the effective input motion which is the response of basement with superstructure, and it is different from foundation input motion, which is massless foundation response and represents kinematic interaction. However, it has the meaning as input for the fixed-base system, which is frequently used in the aseismic design. The input loss effect is clearly recognized in case of the non-dimensional frequency larger than 2. Like the case in which the adjacent building exists, the clear input loss effect is not obtained, so that the factor, which will reduce the input loss effect, should be clarified in future.

STRUCTURAL RESPONSE BASED ON SEISMIC OBSERVATION

In the dynamic response of building where the SSI effect is dominant, the movement of sway and rocking becomes larger than the elastic deformation. Figure 25 shows the transfer function of four buildings based on seismic observation data. These are also averaged ones using more than 10 records. In case of the low rise building, the peak of the transfer function becomes flat, and the distance of the peak position extends between the fixed-base system and the SSI included system.

Figure 26 shows ratio of the sway, rocking and elastic deformation to total displacement for 6 story and 3 story buildings neighboring each other. The sway movement becomes dominant for 3 story building compared to 6 story building. Since the ratio of elastic deformation increases with the frequency, the response distribution of the superstructure varies by the dominant frequency of seismic ground motion. The existence of sway and rocking motion means that the seismic force distribution of the superstructure differs from that of the fixed base condition, and it should be considered in deciding seismic force distribution in aseismic design. These results are also one of the seismic safety margin of low-rise building.

Figure 27 shows the mode shape of both buildings at natural frequency of the 6 story building. Two buildings vibrate in the opposite direction to each other. Dynamic behavior of smaller 3 story building is influenced a lot by larger 6 story building. This is a kind of the cross interaction effect.

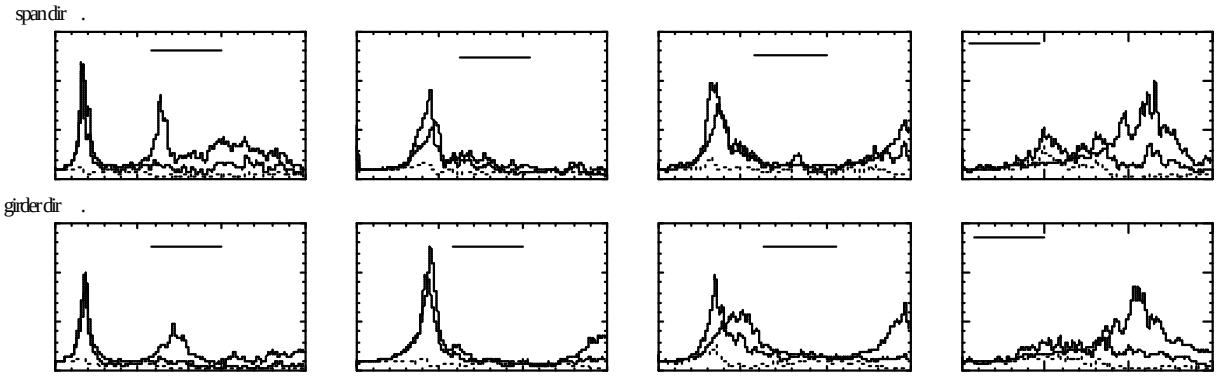

(a) 10F building (b) 4F building (c) 6F building (d) 3F building

Figure 25 Fourier spectrum ratio of four buildings

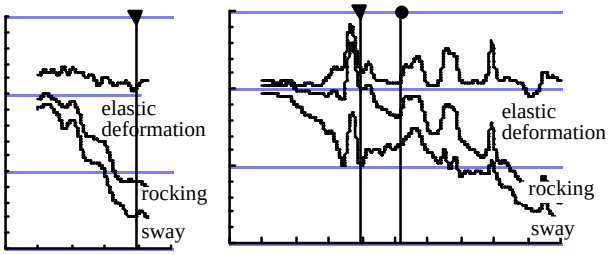

(a) 6F building (b) 3F building

Figure 26 Ratio of elastic deformation, sway and rocking motion for 3 story and 6 story buildings

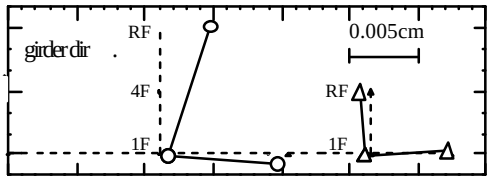

6F building 3F building

Figure 27 Modal shape of neighboring buildings at natural frequency of 6 story building

For four buildings, figure 28 shows the relationship between the maximum acceleration ratio (PRA/PGA=roof / ground surface) and equivalent frequency (PGA/PGV/2p). The amplification factor is different according to the building height. The difference due to the frequency content of seismic ground motion has appeared in the response amplification effect. The result of the figure is well correspondent to the averaged Fourier spectrum ratio shown in figure 25. As a general tendency, response amplification of low-rise building is small compared to taller buildings. Larger amplification is also recognized when the predominant frequency of seismic ground motion is close to natural frequency of the building. Even for the identical soil and building conditions, there is the fluctuation in the response amplification due to the predominant frequency of each seismic ground motion. Therefore we should understand that the response amplification can not be explained only by the resonance of subsurface soil and building.

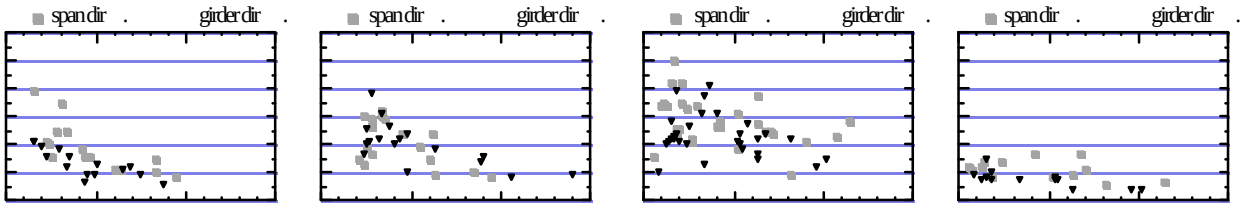

(a) 10F building (b) 4F building (c) 6F building (d) 3F building

Figure 28 Acceleration amplification factor between roof and ground surface for 4 buildings

CONCLUDING REMARKS

The effect of SSI on the dynamic properties of structures was studied analytically and experimentally. As a

result, the dominant effect of SSI was clearly recognized for the low and medium-rise buildings. The main conclusions are as follows:

1) The change of natural period, damping ratio and vibration mode is examined by numerical analyses using simplified model. The results show the reduction of seismic force due to inertia interaction effect especially for low and medium-rise buildings on soft soil.

2) The natural frequency and damping ratio of several low and medium-rise buildings were evaluated through microtremor measurements and seismic observation. The effect of building height and the soil condition on the severity of SSI effect was then studied through comparison of the results. Also, change of natural frequency and damping ratio is examined comparing the results with and without SSI. Also studied was the amplitude dependency of the results which leads to lower frequencies for more severe excitations.

3) The loss in the effective input motion was studied for 6 buildings using more than ten earthquake records. Input loss effect was clearly shown in case of stand-alone large scale building while the effect was not observed when adjacent building exists. Unified input loss property is obtained by defining the non-dimensional frequency using equivalent frequency of seismic ground motion, averaged shear velocity and size of foundation.

4) The dynamic behavior of buildings was studied for 4 buildings with different height. Large amplification was recognized in tall building when the equivalent frequency of seismic ground motion is close to the natural frequency of building. Through the study on the mode shape of building, large sway motion was observed in low-rise building and ratio of the elastic deformation increases with the frequency of input motion. The study on the cross interaction effect of neighboring buildings shows that the dynamic behavior of smaller building is strongly affected by adjacent larger building.

Finally, the authors want to point out the need to increase the quality and quantity of experimental studies on ordinary buildings in order to promote the aseismic design code considering SSI and realize the desired performance based design.

ACKNOWLEDGEMENT

The authors would like to express their thanks to Miss C. Matsuyama, Mr. Y. Mihara and others of Nagoya university, who helped the observation and experiment.

REFERENCES

Architectural Institute of Japan (AIJ), *An Introduction to Dynamic Soil-Structure Interaction* , 1996 (In Japanese)

Fukuwa, N., Ghannad, M.A., Tobita, J., and Nishizaka, R., "Analytical and Experimental Studies on the Effect of Soil-Structure Interaction on Damping, Natural Frequency and Effective Input Motion of Buildings," 1st US-Japan Soil Structure Interaction Workshop, Menlo Park, CA, pp.14-1~14-15, 1998.9

Fukuwa, N., and Tobita, J., "Seismic Observation of Soil Structure Interaction System," The 2nd Symposium on Utilization of Strong Ground Motion Data, AIJ, pp.57-68, 2000.12 (In Japanese)

Fukuwa, N., "Subjects Related to Soil-Structure Interaction in Aseismic Design," The 6th Symposium on Soil Structure Interaction, AIJ, 2001.3 (In Japanese)

Hayashi, Y., Miyakoshi, J., Tasai, A., and Ohno, Y., "Seismic Performance of RC Buildings during Hyogo-ken Nanbu Earthquake," J.Struct. Constr. Eng., AIJ, No.528, pp.135-142, 2000.2 (In Japanese)

Tobita, J., Fukuwa, N., and Yagi, S, "Experimental Evaluation of Dynamic Characteristics of Low and Medium-rise Buildings with Soil-Structure Interaction," 12th World Conference on Earthquake Engineering, Paper No.1343, 8p, 2000.1